High-throughput iSpinach fluorescent aptamer-based real-time monitoring of in vitro transcription

Weitong Qin
1State Key Laboratory of Microbial Metabolism, School of Life Sciences and Biotechnology, Shanghai Jiao Tong University, Shanghai 200240, China

Liang Li
2Hzymes Biotechnology Co., Ltd, Hubei 430010, China

Fan Yang
2Hzymes Biotechnology Co., Ltd, Hubei 430010, China

Siyuan Wang
1State Key Laboratory of Microbial Metabolism, School of Life Sciences and Biotechnology, Shanghai Jiao Tong University, Shanghai 200240, China

Guangyu Yang (yanggy@sjtu.edu.cn)
Shanghai Jiao Tong University Laboratory of Molecular Microbiology: Shanghai Jiao Tong University School of Life Sciences and Biotechnology https://orcid.org/0000-0002-2758-4312

Research

Keywords: in vitro transcription, RNA aptamer, T7 RNAP, real-time detection

Posted Date: July 26th, 2022

DOI: https://doi.org/10.21203/rs.3.rs-1860584/v1

Abstract

In vitro transcription (IVT) is an essential technique for RNA synthesis. Methods for the accurate and rapid screening of IVT conditions will facilitate RNA polymerase engineering, promoter optimization, and screening for new transcription inhibitor drugs. However, traditional polyacrylamide gel electrophoresis (PAGE) and HPLC methods are labor intensive, time-consuming and not compatible with real time analysis. Here we developed an inexpensive, high throughput, and real-time detection method for the monitoring of *in vitro* RNA synthesis so-called STAR (iSpinach aptamer-based monitoring of Transcription Activity in Real-time). STAR has a detection speed at least 100 times faster than conventional PAGE method and provides comparable results in the analysis of *in vitro* RNA synthesis reactions. It also can be used as an easy and quantitative method to detect the catalytic activity of T7 RNA polymerase. To further demonstrate the utility of STAR, it was applied to optimize the initially transcribed region of the GFP gene and several variants were identified with obvious enhanced transcription output. STAR may provide a valuable tool for many biotechnical applications related to the transcription process, which may pave the way for the development of better RNA related enzymes and new drugs.

Introduction

Transcription is one of the most important biological reactions. *In vitro* transcription (IVT) is used in synthesizing mRNA vaccine (Jain, Venkataraman et al. 2021), screening RNA polymerases (Chelliserrykattil and Ellington 2004), analyzing promoter strength (Paul, Stang et al. 2013), and identifying drugs that inhibit transcription reactions (Villicana, Cruz et al. 2014).

Gel electrophoresis is still the mainstream method for analyzing full-length RNA transcripts, the RNA yield and purity can only be analyzed using fluorescent dye or radioisotope after IVT is completed. Transcription by-products, such as abortive products (2–10 nt) (Gong and Martin 2006), double-stranded RNA (Baiersdorfer, Boros et al. 2019), and truncated RNA products, usually lead to smear band when analyzed using PAGE. HPLC and nucleic acid mass spectrometry provide more accurate quantitative tools for RNA analysis (Burcar, Cassidy et al. 2013, Kanavarioti 2019). However, these methods are also suffered from slow speed, low throughput and labor-intensive operations.

The development of fluorescent light-up RNA aptamers (FLAPs) (Ouellet 2016) offers the possibility to directly visualize and track RNA molecules (Su and Hammond 2020). A variety of FLAPs have been developed, they can form special conformations by binding with fluorogen, and generate fluorescence (Chen, Zhang et al. 2019, Dao, Haselsberger et al. 2021). Different aptamers have divergent folding properties and stability, and are also affected by the surrounding RNA conformation, reaction buffer, etc (Trachman, Abdolahzadeh et al. 2018). They have been widely used in measuring gene transcription (Ying, Yuan et al. 2019), observing intracellular RNA localization (Guzman-Zapata, Dominguez-Anaya et al. 2017) and detecting RNA aptamer binding metabolites (Zheng, Zhao et al. 2022), etc. FLAPs have become a powerful tool in RNA research field and offer a possibility to directly observe the RNA synthesis process. Some *in vitro* RNA detection systems have been developed based on FLAPs, Hofer and

colleagues fused the Spinach aptamer to the RNA of interest, the aptamer was cleaved by a hammerhead ribozyme after transcription, resulting in the fluorescence generation (Hofer, Langejurgen et al. 2013), but this method is more complicate. Kartje and colleagues utilized a hybrid DNA template contains double strand promoter and a downstream single strand Broccoli aptamer sequence (Kartje, Janis et al. 2021), however, the fully double strand DNA template were used in IVT, which limits the application of this method. Although these methods provide a way to directly observe the IVT process, both them also suffer from low folding efficiency and poor thermostability owing to the aptamers they chose are not suitable for *in vitro*.

In this study, we established a high-throughput, simple, and sensitive system for monitoring and quantification of RNA synthesis, which we termed STAR (iSpinach aptamer-based monitoring of Transcription Activity in Real-time). We optimized the fundamental conditions including metal ions, ribonucleotide triphosphates, DNA template, pH and reaction temperatures of the STAR. The activity of T7 RNA polymerase was determined using STAR. To further demonstrate the utility of STAR, we also optimized the 5'-UTR sequence from + 1 to + 8 of GFP gene. We found that the STAR can also be used to easily and rapidly quantify the activity of T7 RNAP and optimize the 5'-UTR sequence, which provides a more efficient tool for many techniques using *in vitro* transcription.

Methods

DNA template used for STAR system

The antisense and sense single-stranded DNA templates containing the T7 promoter and a sequence encoding Spinach, tSpinach, Broccoli, tBroccoli, and iSpinach were synthesized by GenScript (Nanjing, China). To prepare the double-stranded DNA template used for the STAR system, the antisense DNA template was annealed to the sense DNA template at a 1:1 M ratio in DEPC-treated water. Samples were heated to 95℃ for 5 min and then slowly cooled to 25℃ in a heating block for over 30 min. The linear DNA template was obtained by PCR amplification for the other DNA templates used in the STAR system. Verification of double-stranded DNA length was performed using agarose gel electrophoresis. The sequences are listed in Table S1.

Determination of the fluorescent intensity of different fluorescent RNA aptamer

The Spinach, tSpinach, Broccoli, tBroccoli and iSpinach RNA transcripts were recovered and purified using PAGE recovery kit (BioTeke, Beijing, China). The 1 μM purified RNA aptamers were treated at 85^{o}C for 5 min to unfold, and then incubated at 25^{o}C for 20 min to promote them to fold into proper structure. The aptamers were next mixed with 80 mM Tris-HCl pH 7.5, 2 mM $MgCl_2$, 100 μM DFHBI and 200 mM K^+ or Na^+ at 1:1 ratio. Then the mixtures were incubated at 25^{o}C for 15 min. The fluorescence intensity produced by different aptamers were determined by microplate reader.

The *in vitro* transcription catalyzed by T7 RNAP used in our study contained 200 mM HEPES, pH 7.5, 30 mM $MgCl_2$, 5 mM NaCl, 20 mM DTT, 0.2 U/μL Murine RNase Inhibitor (hzymes, Hubei, China), 5 mM NTPs mix, 0.002 U inorganic Ppase (Thermo Fisher, USA), 40 U T7 RNAP and 100 μM DFHBI (MCE, Italy). The DNA template of different RNA aptamers (20 nM) were added into the IVT reaction, and then incubated at 37^{o}C for 20 min. Quickly transfer the reaction to ice to stop the reaction. The fluorescence intensity produced by different aptamers were determined by microplate reader (Ex: 469 nm, Em: 501 nm or Ex: 472 nm, Ex: 507 nm) in a 96-well format.

Nucleic acid mass spectrometry

The obtained iSpinach RNA transcripts were purified by PAGE, the target band were cut off from the PAGE gel, and then the band were recovered and purified using PAGE recovery kit (BioTeke, Beijing, China). The RNA was quantified at 50 pmol and analyzed by Matrix assisted laser desorption tandem time of flight mass spectrometry (MALDI TOF 7090).

T7 RNAP enzyme expression and purification

A plasmid expressing T7 RNAP (pQE-80L) was transformed into *E.coli* BL21 (DE3) cells (Transgene, Beijing, China). The cells were cultured in a 1L LB medium supplemented with ampicillin (50 μg/mL) at 37℃ to an OD_{600} of 0.6–0.8 then expression was induced with 1 mM IPTG at 37℃ for an additional 6 h. Cells were pelleted and treated in Buffer A (50 mM Tris-HCl, pH 8.0, 300 mM NaCl, 100 μM EDTA-Na^+, and 3 mM imidazole) and then lysed by high-pressure homogenization. Protein was purified by nickel-affinity chromatography. The resin was washed with Buffer A and Buffer B (50 mM Tris-HCl, pH 8.0, 300 mM NaCl, 10% glycerin, 100 μM EDTA, 10 mM imidazole) and eluted with five bed volumes of Buffer C (50 mM Tris-HCl, 100 mM NaCl, 100 μM EDTA-Na^+, 10% glycerin, 300 mM imidazole). The purified protein was concentrated with an ultrafiltration tube (Millipore, 30 KDa) and exchanged with buffer (20 mM Tris-HCl, pH 8.0, 100 mM NaCl, 100 μM EDTA-Na^+) three times. The concentration was determined by measuring the UV absorbance at 280 nm. The purified T7 RNAP was diluted to a final concentration of 1 mg/mL in storage buffer (50 mM Tris-HCl, pH 8.0, 100 mM NaCl, 100 μM EDTA-Na^+, 1 mM DTT, 75% glycerin) and aliquoted and stored at −80℃.

Real-time fluorescence measurement of *in vitro* transcription

Standard *in vitro* T7 RNAP transcription reaction in our study contained 200 mM HEPES, pH 7.5, 30 mM $MgCl_2$, 5 mM NaCl, 20 mM DTT, 0.2 U/μL Murine RNase Inhibitor (hzymes, Hubei, China), 5 mM NTPs mix, 0.002 U inorganic Ppase (Thermo Fisher, USA), 120 nM DNA template, 40 U T7 RNAP, and 100 μM DFHBI (MCE, Italy). The reaction temperature was typically 37℃. All reactions were performed in 96-well microtiter plates, and the relative fluorescence units (RFU) generated by *in vitro* transcription were measured in real time using a microplate reader. Data processing was performed using the Origin 10 software.

Denaturing polyacrylamide gel electrophoresis (PAGE) of *in vitro* transcription products

After the *in vitro* transcription reaction was completed, samples were treated with 1 U DNase I for 15 min at 37℃ to digest the transcription DNA template. EDTA was added at a final concentration of 60 mM to stop the reaction. The RNA transcripts were mixed with 2×RNA loading dye (NEB, USA) in a 1:1 ratio, boiled at 85℃ for 5 min, then immediately put on ice to stop the reaction. Then 2 μL of the mixed sample was added to 15 % Urea-TBE denaturing polyacrylamide gel. The RNA transcript bands were stained with Gel-red dye for 5 min.

Results And Discussion

Screening fluorescent aptamers suitable for in vitro transcription

The RNA product generated from IVT reaction itself does not generate fluorescence. To develop a simple, fast, low-cost, and real-time detection method for monitoring RNA synthesis, the double strand DNA template for IVT was designed as a sequence contains a common T7 promoter (TAATACGACTCACTATA) and a downstream sequence encoding a fluorescent RNA aptamer (Fig. 1A). Several fluorescent RNA aptamers have been reported, but their fluorescence intensity, thermal stability, and metal ion dependence are quite different (Ouellet 2016). To screen out the most suitable RNA aptamer for real-time fluorescence monitoring *in vitro*, we selected five candidate fluorescent aptamers, Spinach (Paige, Wu et al. 2011), tSpinach, Broccoli (Filonov, Moon et al. 2014), tBroccoli and iSpinach (Autour, Westhof et al. 2016) to measure their relative fluorescence intensity (RFU). Aptamer synthesis and fluorescence were monitored in real-time by a microplate reader in small 50 μL reactions in a 96-well format, and only the full-length products could fold into proper structure and bind to the fluorogen DFHBI to produce fluorescent signal, while the dsRNA and abortive products could not generate fluorescence.

These aptamers were transcribed at 37^{o}C and their fluorescence intensity (RFU) were measured at 25^{o}C in 100 mM metal ions (K^+ or Na^+), considering some aptamers strongly depended on the presence of salt to fold correctly (Filonov, Moon et al. 2014). These results showed that iSpinach had relatively strong fluorescence at excitation wavelengths of 469 nm and 472 nm (Fig. 1B, 1C), and can work in salt free environment (Fig. S2), indicating that iSpinach was more suitable for the IVT reaction, which was performed at 37^{o}C in a reaction not supplemented with K^+. Owing to their low fluorescence *in vitro*, Broccoli, Spinach, tBroccoli and tSpinach were no longer considered in the rest of the study.

To further confirm this result, we analyzed RNA transcripts using denaturing PAGE and nucleic acid mass spectrometry (Fig. 2). We observed the target iSpinach band (72 nt), but there were also two other 3'-extended RNA products (76 nt and 85 nt), which were longer than the full-length product. This result was not surprising, since T7 RNAP has weak RNA-dependent RNA polymerase activity (Gholamalipour, Karunanayake Mudiyanselage et al. 2018). The presence of 3'-extended products does not have much effect on the fluorescence results, because the fluorogen DFHBI only bind with the G-quadruplex motif generated by iSpinach aptamer (Fernandez-Millan, Autour et al. 2017).

Effects of ribonucleotide triphosphates and $MgCl_2$ concentrations on the STAR system

To obtain the best conditions for the STAR system, we decided to optimize its fundamental components, which included the concentration of ribonucleotide triphosphates (NTPs), $MgCl_2$, monovalent ions, T7 RNAP, temperature, and pH. Beginning with our standard conditions, we determined an optimal concentration of iSpinach DNA template to ensure that the amount of DNA template is sufficient. The results showed that the transcription yield reached a plateau when the concentration of DNA template exceeded 120 nM (Fig. S3).

NTPs (Liu, Ke et al. 2020) and $MgCl_2$ (Yin and Steitz 2004) have been known to affect the efficiency of *in vitro* T7 RNAP transcription. Magnesium ions have important roles in nucleotide addition cycles, and NTPs are substrates of IVT, which directly chelate with magnesium. To explore the optimum conditions for the STAR system, we measured the RFU generated at NTP concentrations ranging from 0.5 mM to 6 mM in real time (Fig. 3A). The results showed that the RFU, which represents the RNA yield, increased linearly with an increase in time at all seven NTP concentrations. The RNA yield also showed an upward trend when NTP concentrations ranged from 0.5 mM to 5 mM; However, when the concentration of NTPs exceeded 5 mM, the RNA yield reached a plateau, indicating that 5 mM NTPs should support greater RNA synthesis.

Next, we determined the effect of $MgCl_2$ concentrations ranging from 5 mM to 80 mM on the STAR system under the optimum NTP concentration (Fig. 3B). We found that both limiting and excessive $MgCl_2$ can inhibit the activity of T7 RNAP, and that 40 mM $MgCl_2$ was the optimal concentration for the STAR system. The RNA transcripts were also analyzed by denaturing PAGE, and the RNA yield increased with increasing $MgCl_2$ concentration and reduced when $MgCl_2$ concentrations exceeded 40 mM, consistent with the fluorescence assay results.

Effect of temperature, pH and monovalent ions on the STAR system

Temperature is a key factor affecting *in vitro* transcription efficiency and affinity of iSpinach binding to DFHBI (Autour, Westhof et al. 2016). To identify the optimum temperature for STAR system, we performed transcription experiments at temperatures ranging from 25℃ to 50℃. We observed an increased fluorescence with increasing temperature from 25℃ to 37℃ and reduced fluorescence from 42℃ to 50℃ (Fig. 4A), indicating that iSpinach can form a more stable complex with DFHBI at 37℃. Denaturing PAGE analysis supported these results. The yield of RNA transcripts increased gradually with the increase of temperature, but decreased by 80% at 45°C, and there were no RNA transcripts above 45℃ (Fig. 4A). The optimum temperature was approximately 37℃ and 42°C. These results are consistent with the transcriptional activity of T7 RNAP whose activity is lost above 45℃, indicating that the STAR system can accurately reflect the transcriptional activity of T7 RNAP at different temperatures.

The pH affects the charged state of enzymes and substrates (Rodrigues, Ortiz et al. 2013), thereby affecting enzyme activity. We measured the relative fluorescence intensity of the transcription reaction at different pH values, from 5.5 to 8.5. We found that the STAR system was highly sensitive to pH, and the optimum pH value was approximately 7.5, which was our standard condition (Fig. 4B).

Previous studies have shown that T7 RNAP is highly sensitive to ionic strength of ions such as sodium and chloride ions (Orlov, Ryasik et al. 2018). We screened the NaCl concentrations of STAR system starting from 20 mM to 400 mM, and the results showed that the RNA yield was strongly inhibited by NaCl, the activity decreased above 20 mM, with only 8.3% remaining activity at 160 mM (Fig. 4C). This result indicated that the system did not require the addition of NaCl.

Next, we tested the effects of other monovalent ions on the STAR system. We investigated the effect of 20 mM potassium, cesium, and lithium on the STAR system, and the results showed that the STAR system is not sensitive to any of these monovalent ions and they can even be absent from IVT reactions (Fig. 4D).

Application of STAR in detecting the activity of T7 RNAP

T7 RNAP has widely applications *in vitro* synthesis systems, such as IVT, cell-free transcription/translation system and isothermal amplification systems (Zhang, Huang et al. 2018, Ju, Kim et al. 2021). The catalytic activity of T7 RNAP not only affects the final yield of RNA transcripts but also affects the rate of RNA synthesis. Traditional method of determining the activity of T7 RNAP usually adopts the isotope method, which is prone to radioactive contamination, has high operating costs, making it difficult to achieve high throughput (Padmanabhan, Sarcar et al. 2020). Therefore, establishment of a simple and efficient T7 RNAP activity detection method is helpful for achieving high throughput and automated activity detection, which is one of the urgent problems to be solved in T7 RNAP research field. To demonstrate the application of STAR in detecting the activity of T7 RNAP, we purified T7 RNAP protein and measured the relative fluorescence intensities at T7 RNAP concentrations from 0.78 μg/mL to 50 μg/mL in real-time using STAR.

Our results showed that, at a specific T7 RNAP concentration, the fluorescence intensity produced by STAR is proportional to the time (Fig. 5A); and T7 RNAP concentration has a good linear relationship with the RNA transcripts produced by STAR from 0.75 μg/ mL to 25 μg/mL T7 RNAP (Fig. 5A). Nonetheless, beyond 25 μg/mL, T7 RNAP did not produce substantially greater yields (Fig. 5A). We also measured the fluorescence values generated by different concentrations of commercial T7 RNAP. The lowest concentration of T7 RNAP detected by our STAR method was 0.1 U/μL and the RNA yield reached the plateau phase once the concentration exceeded 10.4 U/μL. These results demonstrate that the STAR system accurately detect the activity of T7 RNAP within a certain concentration range. In addition, the T7 promoter of DNA template can also be replaced, which can be applied to characterize the activity of other types of polymerase, such as SP6 RNA polymerase, T3 RNA polymerase.

Application of STAR in optimizing the initially transcribed region of GFP gene

The complete transcription cycle catalyzed by T7 RNAP involves initiation, elongation, and termination steps (Steitz 2009), the initiation process is the rate-limiting step of the entire transcription. Some studies have shown that the initially transcribed sequence (ITS) (8–10 bp) of DNA template strongly affect the stability of initiation complex (Henderson, Evensen et al. 2019). Inappropriate ITS can cause T7 RNAP to fall off the DNA template, resulting in the production of abortive products (2–10 nt), thereby reducing the yield of transcripts. Therefore, designing a reasonable ITS helps to improve the production of full-length products, and plays an important role in the RNA synthesis such as mRNA vaccines. The ITS has been systematically mutagenized previously, and it has been confirmed that this region affects transcription efficiency (Imburgio, Rong et al. 2000, Conrad, Plumbom et al. 2020). These previous studies provided us with a reliable reference for testing our STAR system.

To investigate the potential utility of STAR, the initially transcribed sequence (5'-UTR) from + 1 to + 8 position of GFP gene was mutated with each mutation representing a single base-pair change to one of the three other base pairs. For example, the first three mutants contained A, C, or T in place of G at the first nucleotide of the 5'-UTR. To ensure that the measured fluorescence intensities were consistent with the levels of synthesized RNA, denaturing PAGE was performed for each transcription reaction.

We observed that transcripts with a G at position + 1 to + 2 were transcribed more efficiently than the three other mutants. Substituting the G to A at position + 1 resulted in a ~ 93% loss in RNA yield, and the G to T mutant at position + 2 resulted in ~ 60% loss in RNA yield, which corresponded very well with the PAGE gel results. To further confirm this result, we also performed truncation experiments at positions + 1 to + 3, transcripts with a G triplet (WT-GGG) were transcribed more robustly compared to other truncated DNA template, which contains two G, one G or none G at positions + 1 to + 3 (Fig. 7). These results are in agreement with previous findings that T7 RNAP is dependent on G at position + 1 to initiate transcription reactions, and with common guidelines for T7 RNAP usage in RNA biology (Passalacqua, Dingilian et al. 2020).

The downstream sequences from + 4 to + 8 also affected transcription efficiency. Substitution of A-T or T-A base pairs with G-C or C-G base pairs at position + 4 resulted in ~ 62% or greater loss in RNA yield. Mutation of + 8A to C and T resulted in 36% and 25% increase in RNA yield. However, the substitution of + 6A with + 6C resulted in ~ 100% loss in RNA yield. These results indicate that this region is more prone to A-T or T-A base pairs, which facilitate the melting of DNA templates (Patwardhan, Lee et al. 2009).

Next, we combined the mutations of DNA templates with increased activity. The product transcribed from 3T4T mutant was 50% higher than that of wild-type (WT-GGG), and 3T8C mutant had little effect (Fig. 7). However, T7 RNAP could not recognize other combined mutations, such as 4T8C, 4T8T, 3T8T (Fig. 7). These results indicated that the initially transcribed region strongly affect the transcriptional activity of T7 RNAP.

The difference in the target gene selected for transcription will also lead to deviation in the transcription results (Conrad, Plumbom et al. 2020). For example, the mutation at position + 5 have little effect on the transcription efficiency of iSpinach, which proves the necessity of optimizing the sequence of the initially transcribed region of different genes. Nonetheless, our results generally agree well with those of previous studies and suggest that the STAR system is reliable and can be used to rapidly optimize the 5’-UTR sequence.

Conclusion

In this study, we describe a high-throughput, simple, and real-time iSpinach aptamer-based method to monitor synthesized full-length RNA *in vitro* that can be easily implemented by most laboratories. We quantified how the efficiency of real-time IVT is affected by its fundamental components, reaction conditions, and initially transcribed region of 5'-UTR sequence. The NTP mix, $MgCl_2$, and NaCl concentrations greatly influenced the total RNA yield, and most results supported and confirmed those of previous IVT studies using PAGE. The STAR system had high thermostability, the optimal reaction temperature was between 37℃ to 42℃, which is very consistent with the conditions of conventional IVT reactions. In conclusion, this method only requires a conventional microplate reader, and the detection speed is at least 100-fold faster than that of traditional PAGE analysis. This provides a new method to rapidly optimize the conditions of IVT, promoter strength, 5'-UTR sequence, and for polymerase screening.

Abbreviations

IVT, *In vitro* transcription; T7 RNAP, T7 RNA polymerase; FLAPs, fluorescent light-up RNA aptamers; DFHBI, 3,5-difluoro-4-hydroxybenzylidene imidazolinone; STAR, iSpinach aptamer-based monitoring of Transcription Activity in Real-time; RFU, relative fluorescence units; PAGE, polyacrylamide gel electrophoresis; NTP, ribonucleotide triphosphate; ITS, initially transcribed sequence.

Declarations

Ethics approval and consent to participate

Not applicable

Consent for publication

Not applicable

Availability of data and materials

The authors declare that all data supporting the findings of this study are available in the paper and its supplementary information files.

Competing interests

The authors declare no competing interests.

Funding

This study was financially supported by National Key R&D Program of China (2018YFE0200501, 2020YFA0907900), National Natural Science Foundation of China (Grant number 32030063).

Authors' contributions

Guangyu Yang conceived the project and designed the experiment. Weitong Qin, Liang Li, Fan Yang and Siyuan Wang carried out the experiments. Guangyu Yang and Weitong Qin wrote the manuscripts. All authors read and approved the manuscript.

Acknowledgements

We are grateful to Prof. Yu Liu from Shanghai Jiao Tong University for providing the protocol of *in vitro* transcription and T7 RNAP enzyme purification.

References

1. Autour, A., E. Westhof and M. Ryckelynck (2016). "iSpinach: a fluorogenic RNA aptamer optimized for in vitro applications." Nucleic Acids Res **44**(6): 2491-2500.
2. Baiersdorfer, M., G. Boros, H. Muramatsu, A. Mahiny, I. Vlatkovic, U. Sahin and K. Kariko (2019). "A Facile Method for the Removal of dsRNA Contaminant from In Vitro-Transcribed mRNA." Mol Ther Nucleic Acids **15**: 26-35.
3. Burcar, B. T., L. M. Cassidy, E. M. Moriarty, P. C. Joshi, K. M. Coari and L. B. McGown (2013). "Potential Pitfalls in MALDI-TOF MS Analysis of Abiotically Synthesized RNA Oligonucleotides." Origins of Life and Evolution of Biospheres **43**(3): 247-261.
4. Chelliserrykattil, J. and A. D. Ellington (2004). "Evolution of a T7 RNA polymerase variant that transcribes 2'-O-methyl RNA." Nat Biotechnol **22**(9): 1155-1160.
5. Chen, X. J., D. S. Zhang, N. Su, B. K. Bao, X. Xie, F. T. Zuo, L. P. Yang, H. Wang, L. Jiang, Q. N. Lin, M. Y. Fang, N. F. Li, X. Hua, Z. D. Chen, C. Y. Bao, J. J. Xu, W. L. Du, L. X. Zhang, Y. Z. Zhao, L. Y. Zhu, J. Loscalzo and Y. Yang (2019). "Visualizing RNA dynamics in live cells with bright and stable fluorescent RNAs." Nature Biotechnology **37**(11): 1287-+.
6. Conrad, T., I. Plumbom, M. Alcobendas, R. Vidal and S. Sauer (2020). "Maximizing transcription of nucleic acids with efficient T7 promoters." Commun Biol **3**(1): 439.
7. Dao, N. T., R. Haselsberger, M. T. Khuc, A. T. Phan, A. A. Voityuk and M. E. Michel-Beyerle (2021). "Photophysics of DFHBI bound to RNA aptamer Baby Spinach." Scientific Reports **11**(1).
8. Fernandez-Millan, P., A. Autour, E. Ennifar, E. Westhof and M. Ryckelynck (2017). "Crystal structure and fluorescence properties of the iSpinach aptamer in complex with DFHBI." Rna **23**(12): 1788-1795.

9. Filonov, G. S., J. D. Moon, N. Svensen and S. R. Jaffrey (2014). "Broccoli: rapid selection of an RNA mimic of green fluorescent protein by fluorescence-based selection and directed evolution." J Am Chem Soc **136**(46): 16299-16308.
10. Gholamalipour, Y., A. Karunanayake Mudiyanselage and C. T. Martin (2018). "3' end additions by T7 RNA polymerase are RNA self-templated, distributive and diverse in character-RNA-Seq analyses." Nucleic Acids Res **46**(18): 9253-9263.
11. Gong, P. and C. T. Martin (2006). "Mechanism of instability in abortive cycling by T7 RNA polymerase." J Biol Chem **281**(33): 23533-23544.
12. Guzman-Zapata, D., Y. Dominguez-Anaya, K. S. Macedo-Osorio, A. Tovar-Aguilar, J. L. Castrejon-Flores, N. V. Duran-Figueroa and J. A. Badillo-Corona (2017). "mRNA imaging in the chloroplast of Chlamydomonas reinhardtii using the light-up aptamer Spinach." Journal of Biotechnology **251**: 186-188.
13. Henderson, K. L., C. E. Evensen, C. M. Molzahn, L. C. Felth, S. Dyke, G. Y. Liao, I. A. Shkel and M. T. Record (2019). "RNA Polymerase: Step-by-Step Kinetics and Mechanism of Transcription Initiation." Biochemistry **58**(18): 2339-2352.
14. Hofer, K., L. V. Langejurgen and A. Jaschke (2013). "Universal aptamer-based real-time monitoring of enzymatic RNA synthesis." J Am Chem Soc **135**(37): 13692-13694.
15. Imburgio, D., M. Q. Rong, K. Y. Ma and W. T. McAllister (2000). "Studies of promoter recognition and start site selection by T7 RNA polymerase using a comprehensive collection of promoter variants." Biochemistry **39**(34): 10419-10430.
16. Jain, S., A. Venkataraman, M. E. Wechsler and N. A. Peppas (2021). "Messenger RNA-based vaccines: Past, present, and future directions in the context of the COVID-19 pandemic." Adv Drug Deliv Rev **179**: 114000.
17. Ju, Y., H. Y. Kim, J. K. Ahn and H. G. Park (2021). "Ultrasensitive version of nucleic acid sequence-based amplification (NASBA) utilizing a nicking and extension chain reaction system." Nanoscale **13**(24): 10785-10791.
18. Kanavarioti, A. (2019). "HPLC methods for purity evaluation of man-made single-stranded RNAs." Scientific Reports **9**.
19. Kartje, Z. J., H. I. Janis, S. Mukhopadhyay and K. T. Gagnon (2021). "Revisiting T7 RNA polymerase transcription in vitro with the Broccoli RNA aptamer as a simplified real-time fluorescent reporter." J Biol Chem **296**: 100175.
20. Liu, Q. J., Y. Q. Ke, Y. H. Kan, X. J. Tang, X. J. Li, Y. J. He and L. Wu (2020). "Compatibility and Fidelity of Mirror-Image Thymidine in Transcription Events by T7 RNA Polymerase." Molecular Therapy-Nucleic Acids **21**: 604-613.
21. Orlov, M. A., A. A. Ryasik and A. A. Sorokin (2018). "Destabilization of the DNA Duplex of Actively Replicating Promoters of T7-Like Bacteriophages." Molecular Biology **52**(5): 686-692.
22. Ouellet, J. (2016). "RNA Fluorescence with Light-Up Aptamers." Front Chem **4**: 29.

23. Padmanabhan, R., S. N. Sarcar and D. L. Miller (2020). "Promoter Length Affects the Initiation of T7 RNA Polymerase In Vitro: New Insights into Promoter/Polymerase Co-evolution." Journal of Molecular Evolution **88**(2): 179-193.
24. Paige, J. S., K. Y. Wu and S. R. Jaffrey (2011). "RNA Mimics of Green Fluorescent Protein." Science **333**(6042): 642-646.
25. Passalacqua, L. F. M., A. I. Dingilian and A. Luptak (2020). "Single-pass transcription by T7 RNA polymerase." Rna **26**(12): 2062-2071.
26. Patwardhan, R. P., C. Lee, O. Litvin, D. L. Young, D. Pe'er and J. Shendure (2009). "High-resolution analysis of DNA regulatory elements by synthetic saturation mutagenesis." Nature Biotechnology **27**(12): 1173-1175.
27. Paul, S., A. Stang, K. Lennartz, M. Tenbusch and K. Uberla (2013). "Selection of a T7 promoter mutant with enhanced in vitro activity by a novel multi-copy bead display approach for in vitro evolution." Nucleic Acids Res **41**(1): e29.
28. Rodrigues, R. C., C. Ortiz, A. Berenguer-Murcia, R. Torres and R. Fernandez-Lafuente (2013). "Modifying enzyme activity and selectivity by immobilization." Chemical Society Reviews **42**(15): 6290-6307.
29. Steitz, T. A. (2009). "The structural changes of T7 RNA polymerase from transcription initiation to elongation." Curr Opin Struct Biol **19**(6): 683-690.
30. Su, Y. C. and M. C. Hammond (2020). "RNA-based fluorescent biosensors for live cell imaging of small molecules and RNAs." Current Opinion in Biotechnology **63**: 157-166.
31. Trachman, R. J., A. Abdolahzadeh, A. Andreoni, R. Cojocaru, J. R. Knutson, M. Ryckelynck, P. J. Unrau and A. R. Ferre-D'Amare (2018). "Crystal Structures of the Mango-II RNA Aptamer Reveal Heterogeneous Fluorophore Binding and Guide Engineering of Variants with Improved Selectivity and Brightness." Biochemistry **57**(26): 3544-3548.
32. Villicana, C., G. Cruz and M. Zurita (2014). "The basal transcription machinery as a target for cancer therapy." Cancer Cell International **14**.
33. Yin, Y. W. and T. A. Steitz (2004). "The structural mechanism of translocation and helicase activity in T7 RNA polymerase." Cell **116**(3): 393-404.
34. Ying, Z. M., Y. Y. Yuan, B. Tu, L. J. Tang, R. Q. Yu and J. H. Jiang (2019). "A single promoter system co-expressing RNA sensor with fluorescent proteins for quantitative mRNA imaging in living tumor cells." Chemical Science **10**(18): 4828-4833.
35. Zhang, Y. C., Q. Y. Huang, Z. X. Deng, Y. C. Xu and T. G. Liu (2018). "Enhancing the efficiency of cell-free protein synthesis system by systematic titration of transcription and translation components." Biochemical Engineering Journal **138**: 47-53.
36. Zheng, G. L., L. Zhao, D. Y. Yuan, J. Li, G. Yang, D. X. Song, H. Miao, L. J. Shu, X. M. Mo, X. D. Xu, L. Li, X. Song and Y. Y. Zhao (2022). "A genetically encoded fluorescent biosensor for monitoring ATP in living cells with heterobifunctional aptamers." Biosensors & Bioelectronics **198**.

Figures

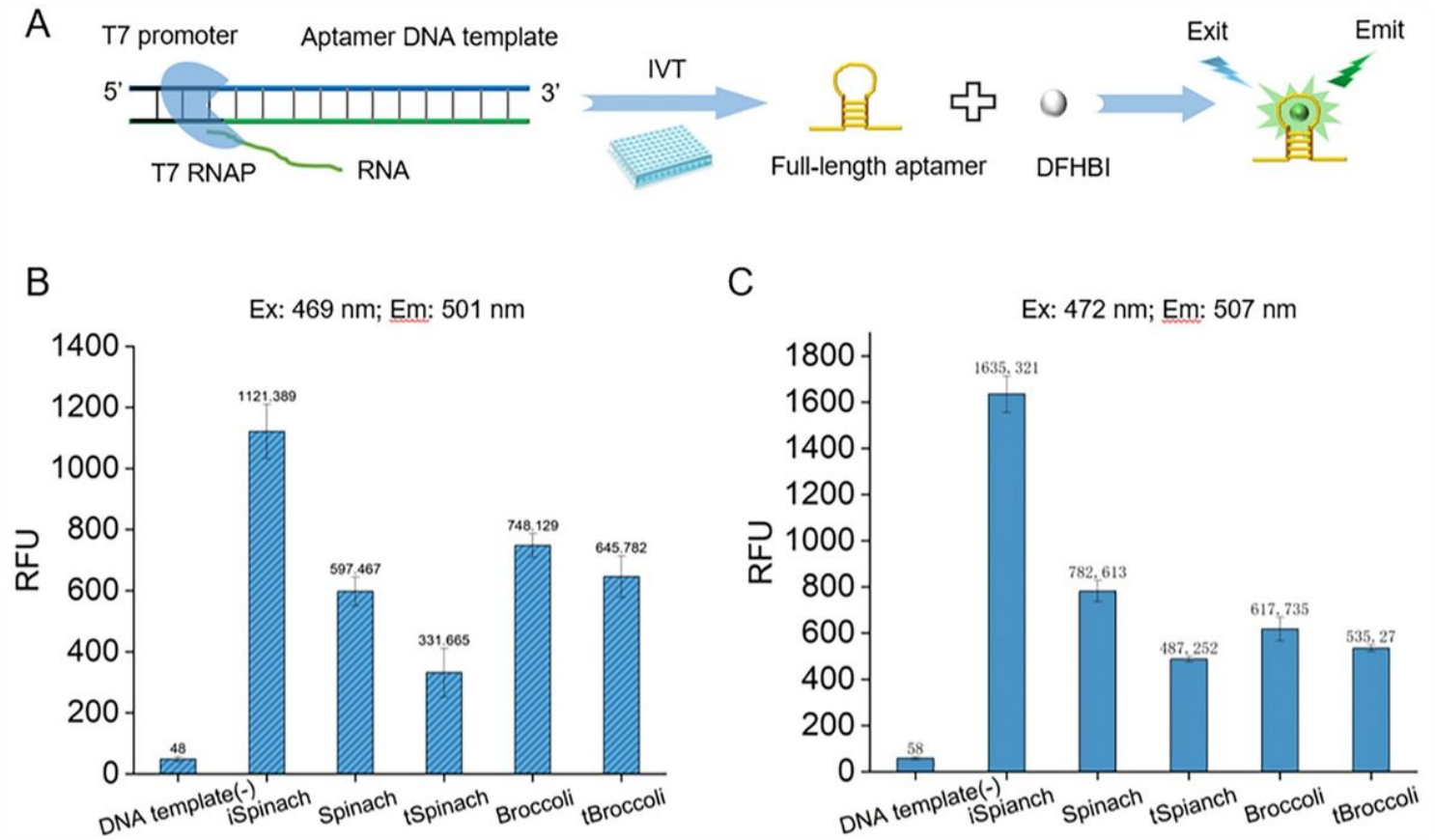

Figure 1

Screening a fluorescent aptamer suitable for *in vitro* transcription. **A** Schematic design of the real-time fluorescent assay method for monitoring the RNA synthesis. The DNA template contains a T7 promoter and downstream sequence encoding fluorescent RNA aptamer. **B** The relative fluorescence units (RFU) generated by five different RNA aptamers were measured under the condition that the excitation wavelength (Ex) was 469 nm and the emission wavelength (Em) was 501 nm. **C** The fluorescence intensities of five different RNA aptamers were measured under the condition that the Ex was 472 nm and the Em was 507 nm. Error bars represent the standard deviation of the triplicate experiments.

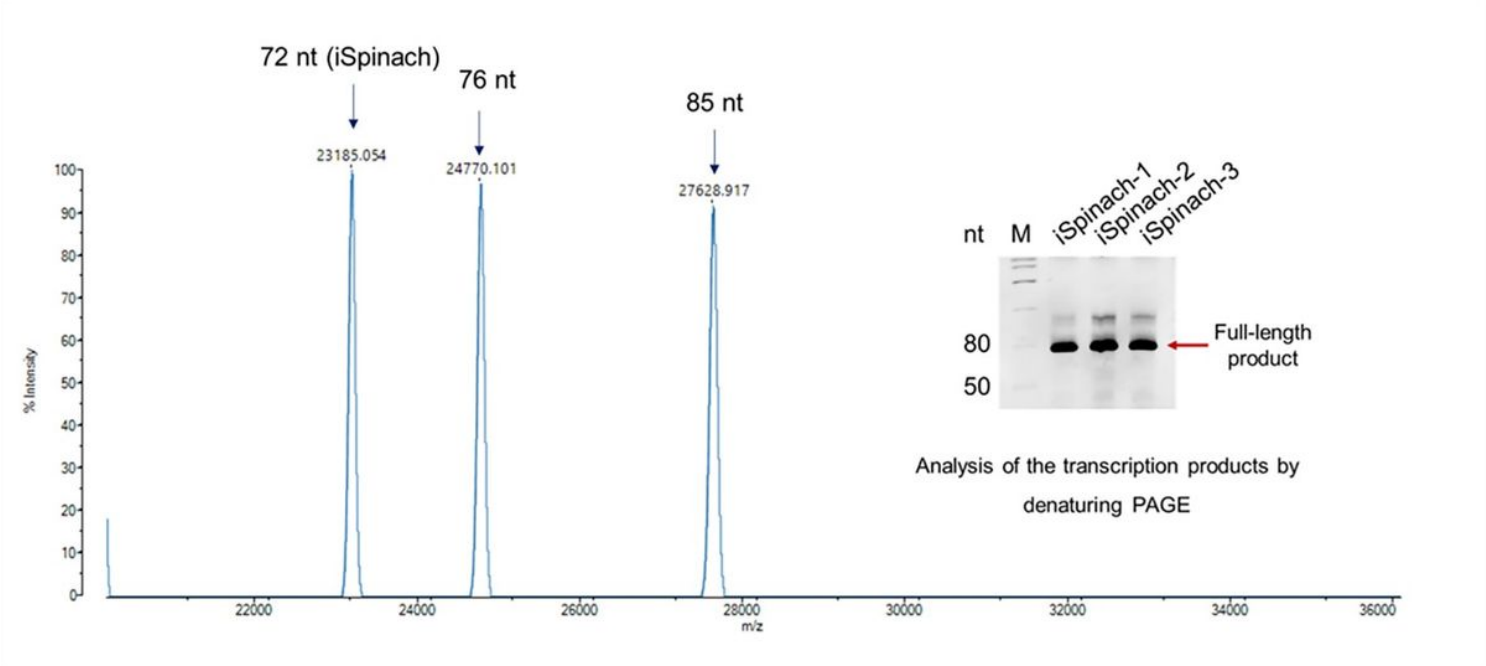

Figure 2

Analysis of iSpinach transcripts by denaturing polyacrylamide gel electrophoresis and nucleic acid mass spectrometry. M represents RNA marker. iSpinach-1, iSpinach-2, and iSpinach-3 represent three different replicates.

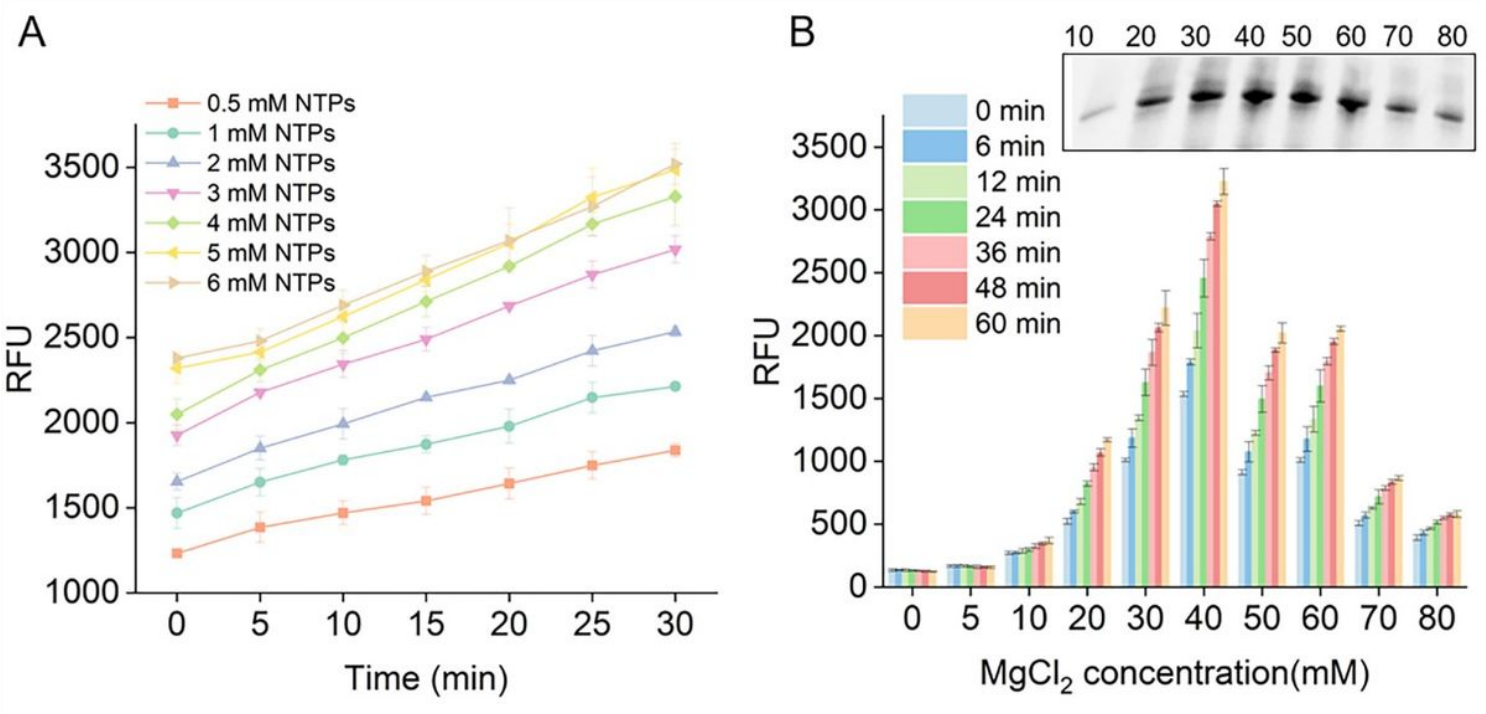

Figure 3

Effects of ribonucleotide triphosphate and $MgCl_2$ concentrations on the STAR system. **A** Effect of NTP concentrations ranging from 0.5 mM to 6 mM. The relative fluorescent units were measured every 5 min. Error bars are standard errors of the mean (SEM). **B** Effect of $MgCl_2$ concentrations ranging from 5 mM to 80 mM. The relative fluorescent units were measured every 6 min. The inset shows the results of denaturing PAGE analysis of the 60 min-transcription products under different $MgCl_2$ concentrations. Error bars represent the standard deviation of the triplicate experiments.

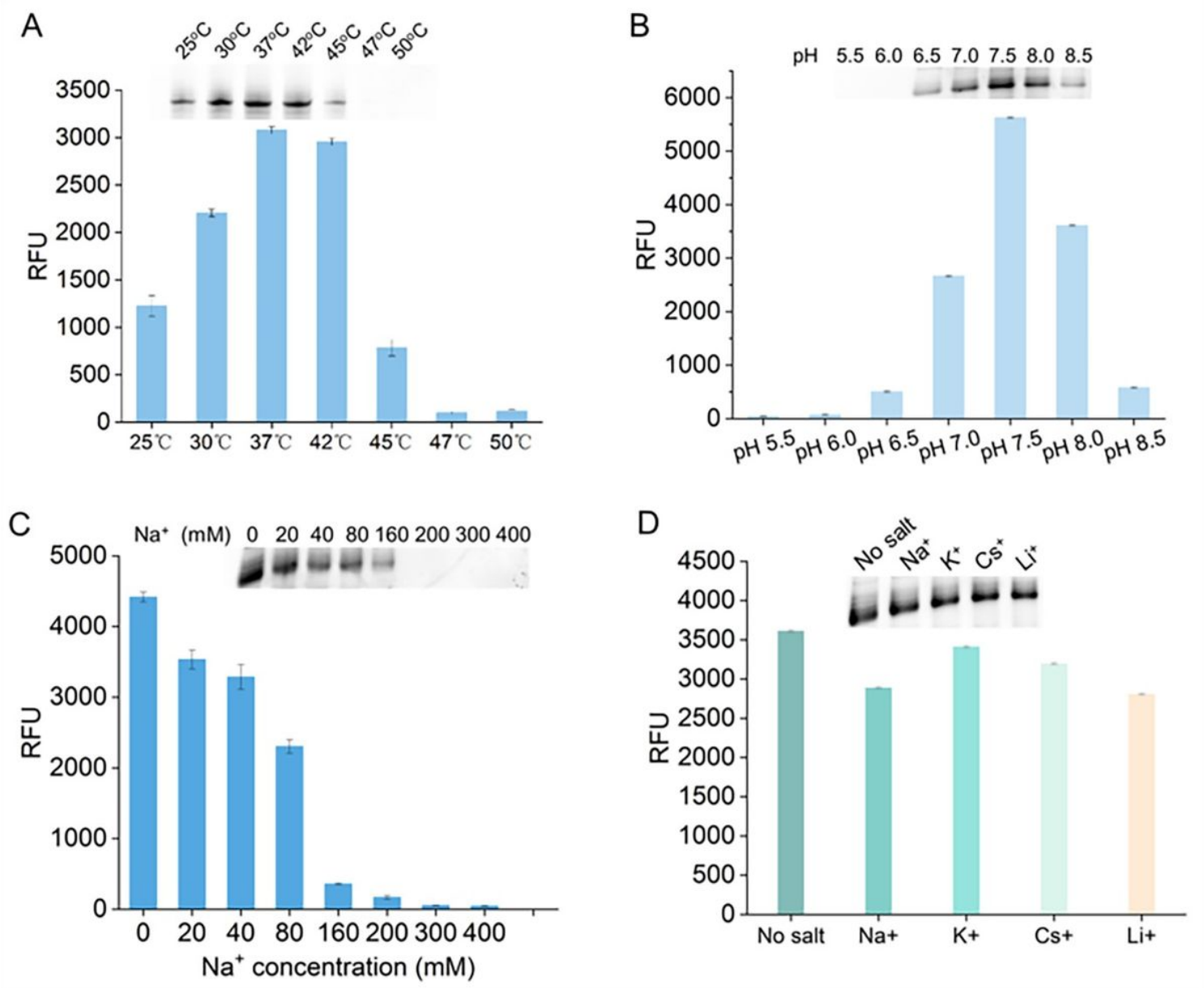

Figure 4

Effect of temperature, pH, and monovalent ions on the STAR system. **A** Relative fluorescence unit at a range of temperatures, the inset shows the results of denaturing polyacrylamide gel electrophoresis analysis of the 120 min transcription products. **B** Relative fluorescence unit for a range of pH values. **C** Relative fluorescence unit for a range of NaCl concentrations. **D** Relative fluorescence unit at 20 mM of

different kinds of monovalent ions. Error bars represent the standard deviation of the triplicate experiments.

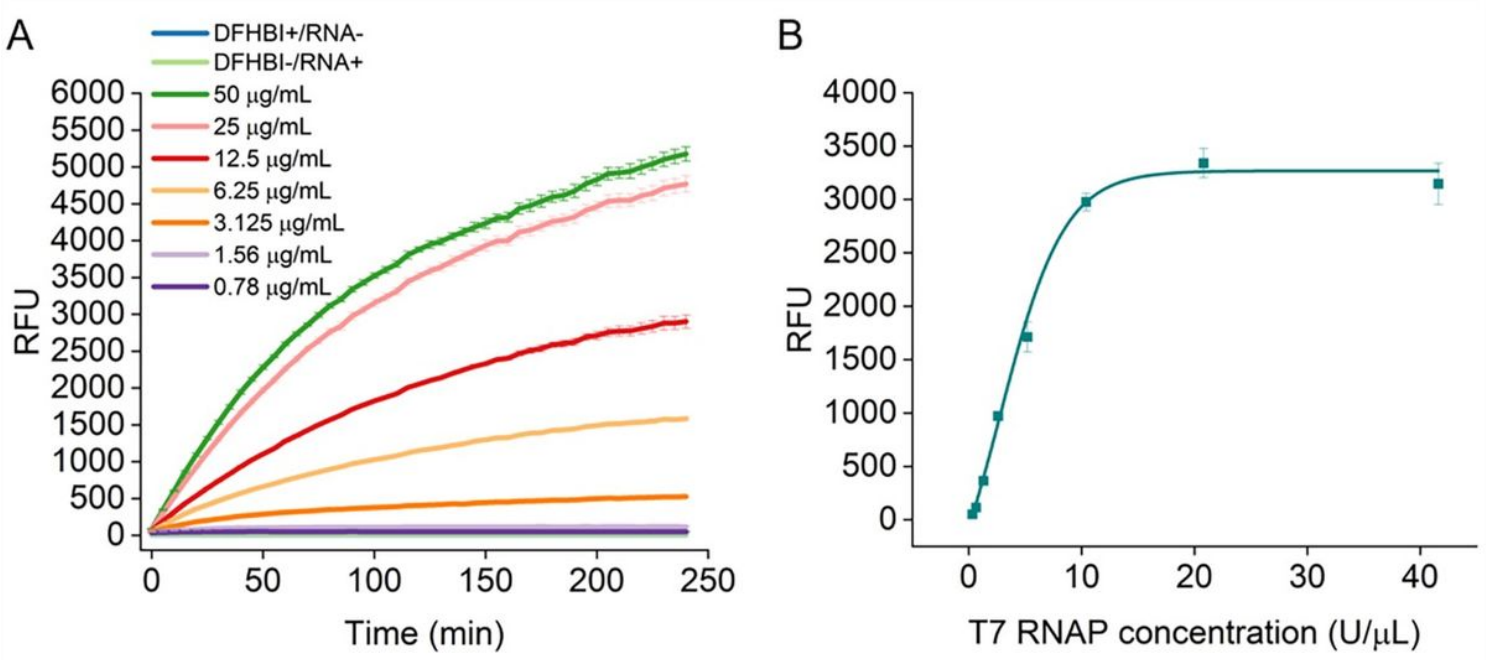

Figure 5

Application of STAR in characterizing the activity of T7 RNAP. **A** Real-time determination of relative fluorescence unit produced by STAR under different concentrations of T7 RNAP. **B** Real-time determination of relative fluorescence unit produced by STAR under different concentrations of commercial T7 RNAP. Error bars represent the standard deviation of the triplicate experiments.

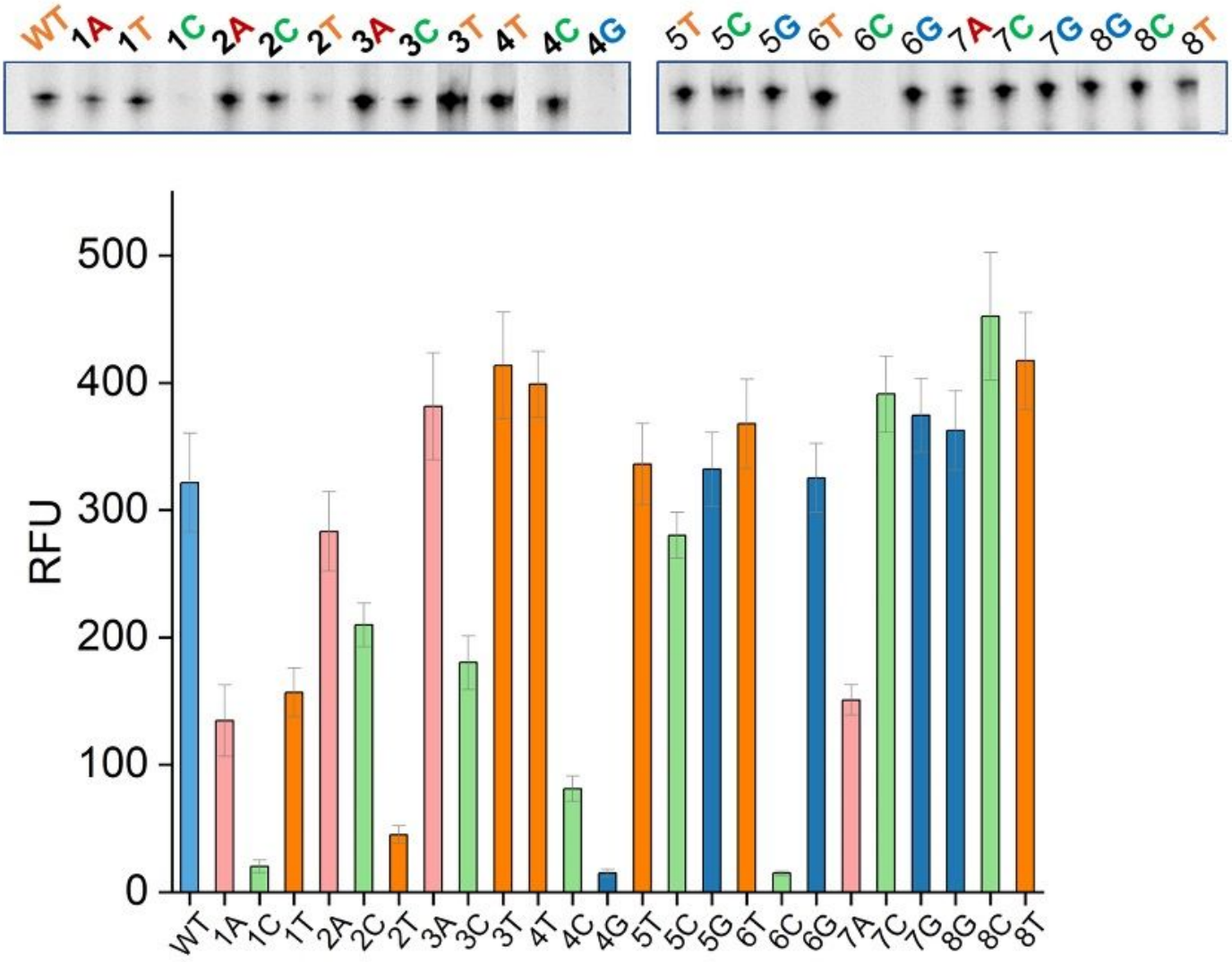

Figure 6

Transcription efficiency of systematically mutated initially transcribed regions of GFP gene quantified by STAR. The effect of substituting three other base pairs at each nucleotide position of 5'-UTR (from +1 to +8) in the DNA template was determined using STAR system. The X-axis represents different mutants, the Y-axis represents the relative fluorescence units. Error bars represent the standard deviation of the triplicate experiments. The inset shows the results of denaturing polyacrylamide gel electrophoresis analysis of the 60 min transcription products.

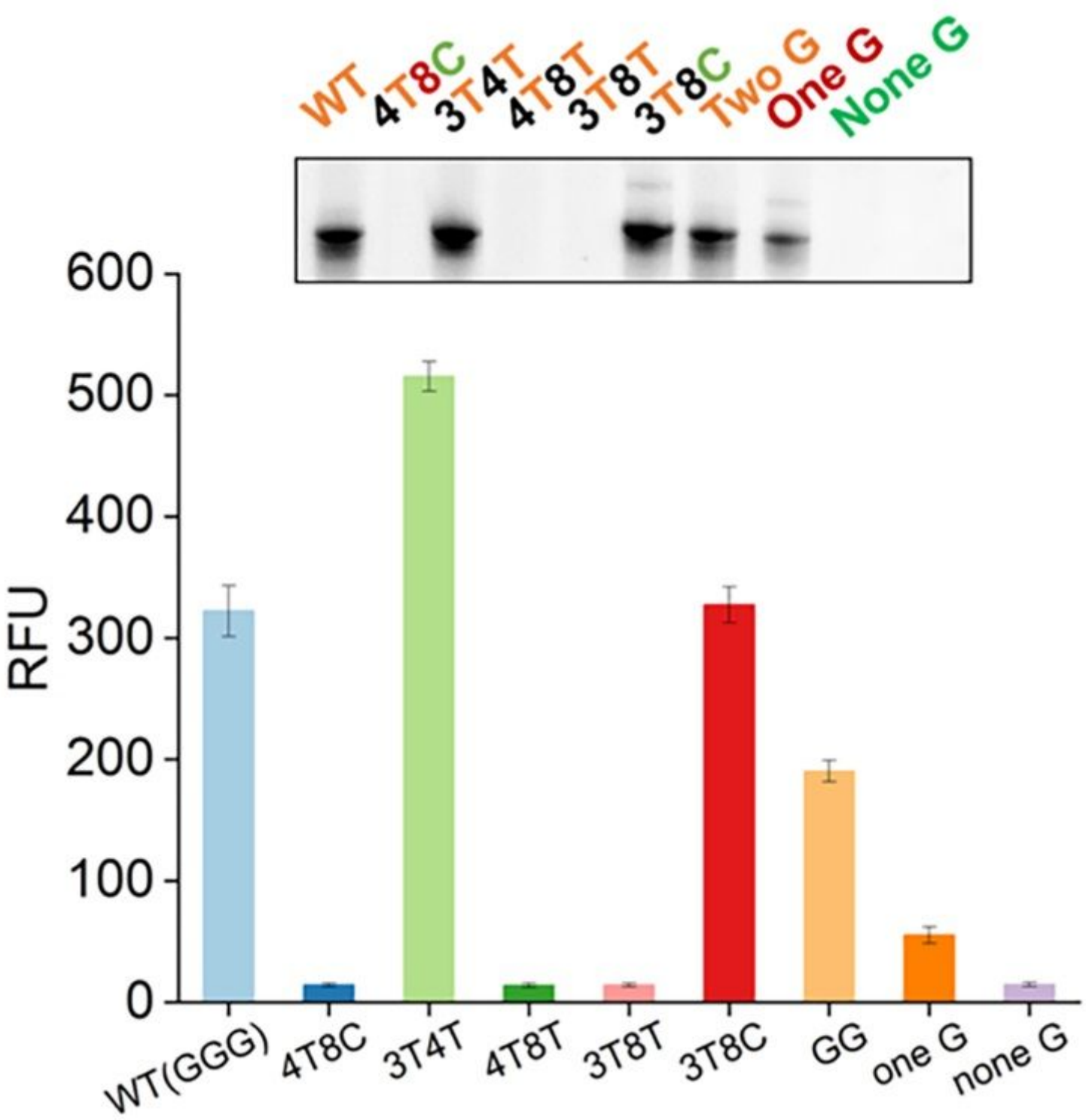

Figure 7

Transcription efficiency of combined mutants and truncated mutants quantified by STAR. The X-axis represents different mutants, the Y-axis represents the relative fluorescence units. Error bars represent the standard deviation of the triplicate experiments. The inset shows the results of denaturing polyacrylamide gel electrophoresis analysis of the 60 min transcription products.

Supplementary Files

This is a list of supplementary files associated with this preprint. Click to download.

- Graphicabstract.docx
- Supplementalmaterials.docx